



Calix[4]arene-Based Clusters with μ_9 -Carbonato-Bridged Co^{II} Cores

Kongzhao Su,^{†§} Feilong Jiang,[†] Jinjie Qian,^{†§} Kang Zhou,^{†§} Jiandong Pang,^{†§} Sulaiman Basahel,[‡] Mohamed Mokhtar,[‡] Shael A. AL-Thabaiti,[‡] and Maochun Hong^{†*}

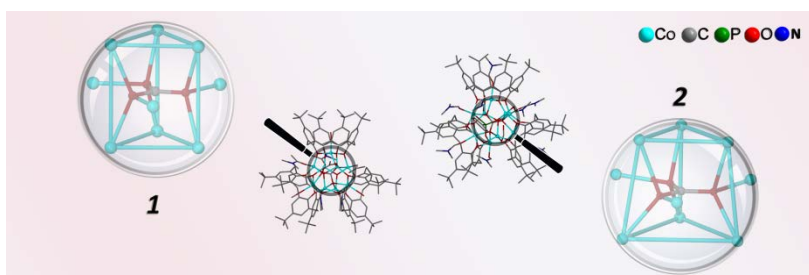
[†]State Key Laboratory of Structural Chemistry, Fujian Institute of Research on the Structure of Matter, Chinese Academy of Sciences, Fuzhou, 350002, China

[‡]Department of Chemistry, Faculty of Science, King Abdulaziz University, Jeddah, 21589, Saudi Arabia

[§]University of the Chinese Academy of Sciences, Beijing, 100049, China

Received on: 14-Jan-2014

ABSTRACT



Two discrete complexes, $[\text{Co}^{\text{II}}_9(\text{TBC}[4])_3(\mu_9\text{-CO}_3)(\mu\text{-H}_2\text{O})_3(\mu_3\text{-OH})_2(\mu\text{-CH}_3\text{COO})_2(\text{DMA})_4] \cdot 3\text{H}_2\text{O} \cdot 2\text{CH}_3\text{OH}$ (**1**), $[\text{Co}^{\text{II}}_9(\text{TBC}[4])_3(\mu_9\text{-CO}_3)(\mu_3\text{-OH})(\mu\text{-HCOO})(\text{O}_3\text{PPh})(\text{DMF})_8] \cdot 2\text{H}_2\text{O} \cdot \text{CH}_3\text{OH}$ (**2**) (TBC[4] = *p*-tert-butylcalix[4]arene, DMA = N,N'-dimethylacetamide, DMF = N,N'-dimethylformamide), have been solvothermally obtained and structurally characterized by single-crystal X-ray diffraction analyses and powder X-ray diffraction. Complex **1** capped by three TBC[4] ligands possesses a tri-capped trigonal prismatic Co^{II}_9 core housing a μ_9 -carbonato anion. When auxiliary phosphonate ligand is introduced into the reaction, complex **2** is obtained with an obvious geometrical change in the metallic core moving from a regular tri-capped trigonal prism in **1** to a distorted one in **2**. What is more, this work represents the first two examples of $\mu_9\text{-CO}_3^{2-}$ bridged paramagnetic metal clusters reported in the literature. Magnetic measurements reveal that both of the complexes show spin-glass behavior.

Keywords: Calix[4]arene, Cluster, Magnetism, Spin-glass

INTRODUCTION

The design and synthesis of novel polynuclear metal clusters have become one of the most active field in coordination

chemistry and material chemistry in the past few decades, not only due to their intriguing structures¹⁻³ but also their potential technological applications in magnetism,⁴⁻⁶ catalysis,^{7,8} conductivity,⁹ nonlinear optical material¹⁰ and gas adsorption and storage.^{11,12} Recently, a large number of polymetallic clusters with interesting geometries and novel properties have been obtained by employing bridging anions such as OH⁻, NO₃²⁻, C₂O₄²⁻, X⁻ (X = F, Cl, Br, I) or *in situ* generated anions such as CO₃²⁻, PO₄³⁻, tetrazolate under hydro-/solvo-thermal conditions.¹³⁻¹⁵ Among these anions, the carbonate anion with three donor oxygen atoms has been proved to be an excellent

Corresponding Author: Maochun Hong

Email: hmc@fjirsm.ac.cn

Tel; +86-591-83792460

Cite as: *Int Res Adv*, 2014, 1(1), 14-21 or as *Inorg. Lett.* 2014,1(1), 1-8.

©IS Publications

bridging anion showing a variety of coordination modes. Thus many carbonato-bridged transition metal (TM), lanthanide metal (LnM) and 3d-4f heterometallic clusters with different nuclearity, for example, Co₅, Dy₆, Ni₈, Gd₈, Mn₁₄, Zn₂Dy₂ and Cu₁₅Gd₇ have been obtained.¹⁶⁻²¹ It is also found that different coordination modes of the carbonato anions can markedly influence cluster formation, which often lead to a large diversity in magnetic properties. Generally speaking, there are three main ways to introduce the carbonate anion for those reported carbonato-bridged complexes: (i) fixing atmospheric carbon dioxide,^{22,23} (ii) inducing by *in situ* generated reactions,^{24,25} (iii) preparing from carbonate salts.²⁶ Very recently, our group has synthesized a series of polynuclear Ni^{II}₈ clusters based on thiacalix[4]arenes with *in situ* generated carbonato anions,²⁵ and cationic Mn^{II}₂₄ coordination cages, heterometallic thiacalix[4]arene-supported Na₂Ni^{II}₁₂Ln^{III}₂ clusters (Ln = Tb and Dy) by directly introducing carbonate salts.^{27,28}

On the other hand, calix[4]arenes are macrocyclic ligands composed of aryl units, linked by methylene bridges. It is found that calix[4]arenes show good abilities in the construction of metal clusters owing to their four inherent lower-rim phenolic oxygen atoms, which can be used to bind either TM or LnM.²⁹⁻³² So far, to construct polynuclear complexes with calix[4]arene has attracted increasing attention. In this respect, Dalgarno's group has reported several complexes with interesting magnetic properties. For example, they have reported calix[4]arene-based Mn^{III}₂Mn^{II}₂ SMMs,²⁹ Mn^{III}₄Gd^{III}₄ magnetic cooler³⁰ and ferromagnetic Mn₅ cage by introducing complementary ligands.³¹ Moreover, thiacalix[4]arenes and their oxidized derivatives (sulfinyl-/sulfonyl-calix[4]arene) with additional donor atoms around the bridges have also been used in the formation of novel polymetallic complexes.³³⁻³⁵ It should be noted that compared to methylene-bridged calix[4]arenes, these additional donor atoms often lead to dramatically different cluster motifs by participating in the coordination chemistry of the resulting complexes.

Our group has focused on constructing new polymetallic clusters by utilizing calixarene ligands that may exhibit interesting magnetic properties.³⁶⁻³⁹ Previously, our group and Liao's group have reported a family of thiacalix[4]arene-based cobalt complexes, 14 of whose magnetic properties have been investigated and show dominant antiferromagnetic interactions between spin carriers.^{37-39,40-46} To our best of knowledge, there is only one reported trinuclear Co₃ cluster supported by two calix[4]arene ligands, but its magnetic behavior has not been investigated.⁴⁷ For the above reasons, we have tried to use *p*-tert-butylcalix[4]arene (TBC[4]) ligand in preparing new cobalt clusters to compare the magnetic behavior with these thiacalix[4]arene-based cobalt clusters. Fortunately, we have successfully obtained two novel calix[4]arene-based cobalt(II) clusters. Notably, [Co^{II}₉(TBC[4])₃(μ₉-CO₃)(μ₃-OH)(μ₃-HCOO)(O₃PPh)(DMF)₈]•2H₂O•CH₃OH (**1**) (DMA = *N,N'*-dimethylacetamide), possesses a tri-capped trigonal prismatic Co^{II}₉ core housing a μ₉-CO₃²⁻ anion, which is directly employed sodium bicarbonate as the source of carbonato anion. When complementary phosphate ligand is introduced into the

reaction, [Co^{II}₉(TBC[4])₃(μ₉-CO₃)(μ₃-OH)(μ₃-HCOO)(O₃PPh)(DMF)₈]•2H₂O•CH₃OH (**2**) (DMF = *N,N'*-dimethylformamide) is obtained with a distorted tri-capped trigonal prismatic core, where the *in situ* generated CO₃²⁻ anion is different from one in complex **1**. Determined by bond-valence-sum calculations, all the metal ions in both complexes are at a +2 oxidation state as required for the charge balances (Tables S1 and S2 in the Supporting Information, SI).⁴⁸ Herein we report the syntheses, structures and magnetic properties of both of the title complexes.

EXPERIMENTAL SECTION

Materials and Measurements. Starting material, *p*-tert-butylcalix[4]arene ligand, was prepared according to published method.⁴⁹ All other chemicals and solvents were purchased from commercial sources and used without further purification. Elemental analyses (C, H, and N) were performed on a German Elementary Varil EL III instrument. IR spectra were obtained as KBr pellets with a Magna 750 FT-IR spectrometer. Powder X-ray diffraction (PXRD) measurements were recorded at room temperature by a RIGAKU-DMAX2500 X-ray diffractometer using Cu Kα radiation (λ = 0.154 nm). Thermogravimetric analysis (TGA) curves were obtained on a NETZSCH STA 449C thermal analyzer. Magnetic susceptibility measurements performed on microcrystalline sample, using a Quantum Design PPMS-9T and MPMS-XL systems. All experimental magnetic data were corrected for the diamagnetism of the sample holders and of the constituent atoms according to the Pascal's constants.

Syntheses of Complexes 1-2. Complex 1. Purple block-shaped crystals of **1** were obtained from the mixture of TBC[4] (0.15 mmol, 100 mg), Co(OAc)₂•4H₂O (0.4 mmol, 100 mg) with NaHCO₃ (0.1 mmol, 8.4 mg) in DMA/CH₃OH (5/5mL). The resulting solution was sealed in a 25 mL Teflon-lined bomb at 120 °C for 3 days, then cooled slowly at 4 °C h⁻¹ to room temperature. X-ray quality crystals were isolated by filtration, washed with DMA/CH₃OH (1:1, v/v) and air dried. Yield 68% based on ligand. Elemental analysis (%) calculated for dried sample **1**, C₁₅₅H₂₁₆N₄O₃₃Co₉: C, 58.29; H, 6.82; N, 1.76. Found C, 57.89; H, 6.64; N, 1.69. IR (KBr disk, ν / cm⁻¹): 3614 (w), 3427 (w), 3043 (w), 2954 (s), 1616 (s), 1453 (s), 1356 (m), 1290 (s), 1200 (s), 1127 (m), 1020 (w), 907 (w), 873 (m), 801 (m), 744 (w), 671 (w), 613 (w), 516 (m). PXRD measurement indicated the crystalline phase purity of **1**. (Figure 1a).

Complex 2. Purple block-shaped crystals of **2** were obtained from the mixture of TBC[4] (0.1 mmol, 65 mg), Co(OAc)₂•4H₂O (0.4 mmol, 100 mg) with PhPO₃H₂ (0.05 mmol, 8 mg) in DMF/CH₃OH (5/5mL). The resulting solution was sealed in a 25 mL Teflon-lined bomb at 120 °C for 3 days, then cooled slowly at 4 °C h⁻¹ to room temperature. X-ray quality crystals were isolated by filtration, washed with DMA/CH₃OH (1:1, v/v) and air dried. Moreover, by the direct adding of HCOONa•2H₂O (0.1 mmol, 10mg) in the mixture, complexes **2** can also be obtained. Yield 65% based on ligand. Elemental analysis (%) calculated for dried sample **2**, C₁₆₅H₂₂₇N₈O₃₂PCo₉: C, 58.36; H, 6.74; N, 3.30. Found C, 58.82; H, 6.49; N, 3.14. IR (KBr disk, ν / cm⁻¹): 3614 (w), 3418 (w), 3044 (w), 2954 (s), 1665 (s), 1576 (w), 1453 (s), 1356 (m), 1298 (s), 1201 (s), 1128 (m), 1095

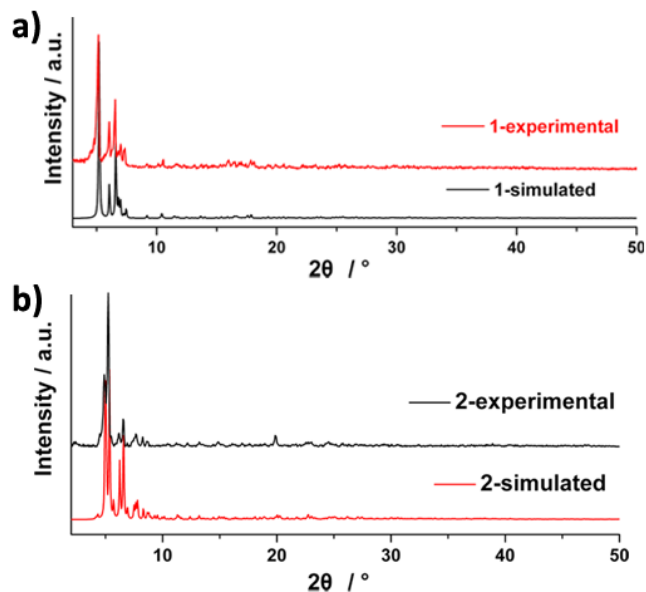


Figure 1. PXRD of complexes **1** and **2**.

(m), 1013 (w), 907 (w), 866 (w), 809 (m), 744 (m), 671 (w), 516 (m). PXRD measurement indicated the crystalline phase purity of **2**. (Figure 1b).

X-ray Data Collection and Structure Determination. The X-ray intensity data for single crystals of **1** and **2** (CCDC number: 979033 and 979034) were collected on a Rigaku Saturn 70 CCD diffractometer at 293 K and a Rigaku Saturn 724+ CCD diffractometer at 120 K equipped with graphite monochromated Mo-K α radiation ($\lambda = 0.71073 \text{ \AA}$) by using the ω -scan mode, respectively. All absorption corrections were applied using the *CrystalClear* program.⁵⁰ Both of the crystal structures were solved by direct methods and refined by full-matrix least-squares fitting on F^2 by the *SHELXTL-97* program.⁵¹ All the non-hydrogen atoms, except some badly disordered atoms and some isolated solvent molecules, were refined anisotropically. The positions of hydrogen atoms on the organic ligands were generated geometrically onto the specific atoms and refined isotropically with fixed thermal factors. Disorder was observed in three oxygen atoms with the same occupancy factor of 0.5 in **1**. Moreover, diffuse electron density associated with solvent molecules of crystallization and hydrogen atoms on coordinated water and solvent molecules cannot be generated but they were included in the molecular formula directly. Moreover, the high R_1 and wR_2 factor both of the complexes might be due to the disorder of the solvent molecules and the weak crystal diffractions. Therefore, the “SQUEEZE” method⁵² was implemented to the crystal data, which had dramatically improved the agreement indices.

Table 1. Crystal Data and Data Collection and Refinement Parameters for 1-2

	1	2
formula	C ₁₅₅ H ₂₁₆ N ₄ O ₃₃ Co ₉	C ₁₆₅ H ₂₂₇ N ₈ O ₃₂ PCo ₉
formula weight	3200.89	3396.03
temperature (K)	293	120
crystal system	Monoclinic	triclinic
space group	C2/c	$P\bar{1}$
<i>a</i> (Å)	27.395(8)	19.726(6)
<i>b</i> (Å)	23.659(6)	21.295(6)
<i>c</i> (Å)	31.59(1)	23.660(7)
α (°)	90.00	95.816(1)
β (°)	112.690(3)	113.497(4)
γ (°)	90.00	101.789(2)
<i>V</i> (Å ³)	18886(9)	8735(4)
<i>Z</i>	4	2
<i>D_c</i> /Mg/m ³	1.1231	1.2910
μ /mm ⁻¹	0.829	0.906
data collected	59354	76545
unique data	16525	30523
parameters	938	1954
GOF on F^2	1.062	1.042
R_1^a [$I > 2\sigma(I)$]	0.0820	0.0758
wR_2^b	0.2347	0.2160

$$^a R_1 = \sum ||F_o| - |F_c|| / \sum |F_o|. \quad ^b wR_2 = \{ \sum [w(F_o^2 - F_c^2)^2] / \sum [w(F_o^2)] \}^{1/2}$$

RESULTS AND DISCUSSION

Crystal structures. Single-crystal X-ray diffraction analysis reveals that complex **1** crystallizes in the monoclinic system with space group C2/c. The metallic core of **1**, capped by three TBC[4] ligands, describes a Co^{II}, tri-capped trigonal prism housing a μ_3 -CO₃²⁻ anion, as can be seen from Figure 2. Within **1**, the trigonal prism is constructed by Co2, Co3, Co4 and their symmetry equivalents Co2A, Co3A and Co4A ions, while the three square faces are capped by Co1, Co1A and Co5 ions. The “upper” triangular face is linked by a μ_3 -OH (O9), with the neighboring Co2...Co3A, Co2...Co4 and Co3A...Co4 distances being of 3.480, 3.503 and 3.514 Å, respectively, and

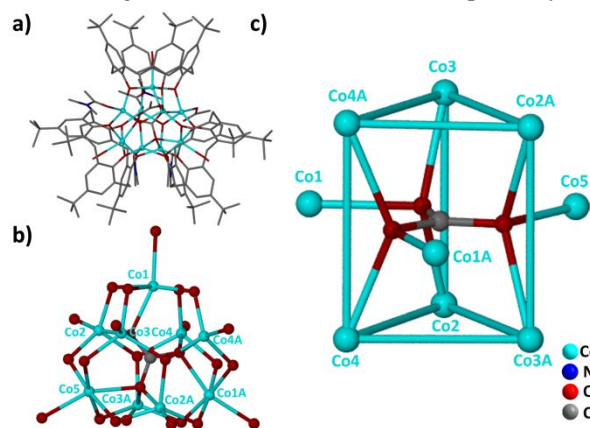


Figure 2. (a) Molecular structure of complex **1**. The hydrogen atoms and isolated solvent molecules are omitted for clarity. (b) Coordination environment of the metals in **1**. (c) The tri-capped trigonal prism Co^{II} core within **1**. Symmetry code: (A) 1-x, y, 1/2-z.

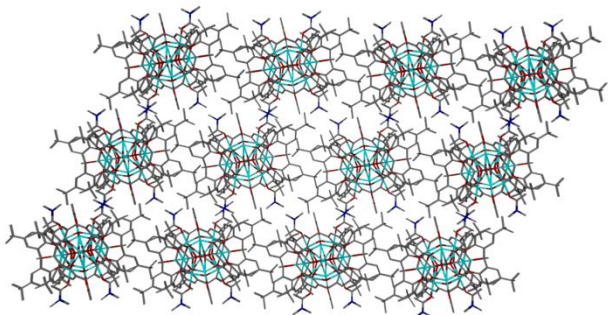


Figure 3. Extended structure of complex **1** showing self-assembly into a skewed bilayer array view along *b* axis. The hydrogen atoms and isolated solvent molecules are omitted for clarity.

with Co2-O9-Co4, Co2-O9-Co3A and Co3A-O9-Co4 angles being 113.25°, 114.79° and 114.22°, respectively. Moreover, the distance between the triangular faces is about 4.159 Å, and the Co···Co distances between the caps and adjacent square faces are in the range of 3.328-3.361 Å. Moreover, complex **1** has a crystallographic two-fold axis so that there are five different crystallographic unique positions for the metal atoms. Among them, the cobalt ion in the vertex of the trigonal prism is five-coordinated in a distort trigonal bipyramid geometry, bonded by two phenoxo oxygen atoms, one μ_3 -OH, one carbonato oxygen atom, and one other components (one oxygen atom from acetic anion for Co5, and one from DMF for Co2 and Co3, respectively), while the other cation situated at the cap is six-coordinated in a distort octahedral coordination environment with four phenoxo oxygen atoms, one carbonato oxygen atom, and one water oxygen. Each oxygen of the carbonato anion bonds to three cobalt cations in a μ_3 -bridging mode. It should be mentioned that this coordination mode is rare according to the search of the Cambridge Structural Database for coordination complexes.^{53,54} As can be seen from Figure 3, the extended structure of **1** is assembled by the stacking of Co^{II} entities, which further construct into skewed bilayer array *via* weak interactions such as van der Waals, π ··· π and hydrogen-bonding interactions. The interstices of the lattice are filled with isolated solvent CH₃OH and water molecules.

When auxiliary phosphonate ligand is introduced into the reaction, complex **2** is obtained with an obvious geometrical change in the metal skeleton moving from a regular tri-capped trigonal prism in **1** to a distorted one in **2**, because one μ_3 -OH has been replaced by a larger μ_3 -bridging phosphonate ligand in one of the triangular faces (Figure 4). It should be noted the phosphonate is an excellent ligand for making polymetallic complexes, because their different anionic forms can adopt various coordination modes. Within **2**, the neighboring Co···Co distances of the “upper” triangular face linked by a μ_3 -OH (O31) range from 3.435 to 3.448 Å, which are shorter than those in the “lower” triangular face capped by a phosphonate ligand range from 4.447 to 4.492 Å, and the Co2-O31-Co5, Co2-O31-Co8 and Co5-O31-Co8 angles are 114.73°, 114.15° and 113.46°, respectively. In addition, the distance between the

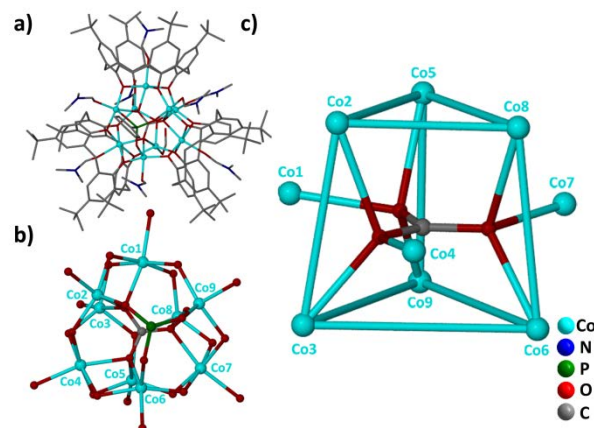


Figure 4. (a) Molecular structure of complex **2**. The hydrogen atoms and isolated solvent molecules are omitted for clarity. (b) Coordination environment of the metals in **2**. (c) The tri-capped trigonal prism Co^{II}_9 core within **2**.

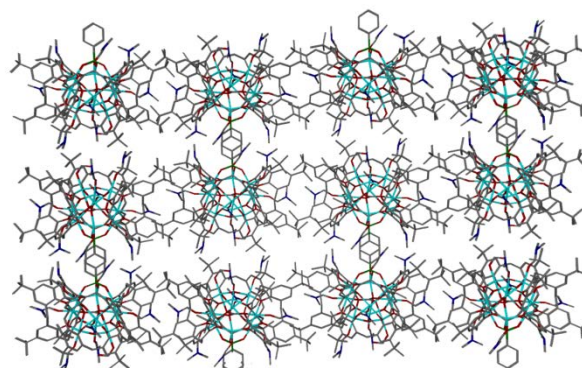


Figure 5. Extended structure of complex **2** showing self-assembly into a bilayer array with ABAB····· mode fashion view along *b* axis. The hydrogen atoms and isolated solvent molecules are omitted for clarity.

abovementioned faces is about 3.861 Å, which is shorter than that in **1**, and the Co···Co distances between the caps and adjacent square faces are in the range of 3.192-3.544 Å, which is shorter than those in **1**. Compared with complex **1**, it is obvious that the neighboring Co···Co distances of the “upper” triangular face in **2** are close to those of **1**, while the ones of the “lower” triangular face in **2** are much longer. Instead of the monoclinic system with space group *C2/c* of **1**, complex **2** crystallizes in the triclinic system *P-1*, and all nine cobalt centers are crystallographically independent. The upper triangular face sites (Co2, Co5 and Co8) are five-coordinated in a square-pyramid geometry with two phenoxo oxygen atoms, two carbonato oxygen atoms, one bridging hydroxide oxygen and one other component (one oxygen atom from formate anion for Co5, and one DMF for Co2 and Co8, respectively), while the lower triangular face sites (Co3, Co6 and Co9) are five-coordinated in a trigonal-bipyramid geometry with two phenoxo oxygen atoms, one phosphonate oxygen atom, one carbonato oxygen atom and one oxygen atom from DMF. Moreover, three cap sites (Co1, Co4 and Co7) are six-coordinated with four oxygen atoms from one fully

deprotonated TBC[4] ligand, one oxygen atom from carbonato anion and one from DMF generating distort octahedral geometry. It should be pointed out that formate and carbonato anions in the structure of **2** are originated from the decarbonation of DMF with solvothermal technique, which also have been documented as excellent bridge anions for constructing polynuclear metal complexes.^{25,38} Examination of the extend structure reveals that complex **2** exhibits a layer structure stacked by the Co^{II} entities in an ABAB..... mode fashion through supramolecular stacking interactions (Figure 5), which is different to the skewed bilayer array observed in the abovementioned complex **1**.

Although there has been a report on calix[4]arene-supported tri-capped trigonal prismatic Cu^{II} clusters, those clusters are cations carried an overall +1 charge, and the charge balance is supplied by a $[\text{Cu}^{\text{I}}\text{Cl}_2]^-$ or NO_3^- anion.⁵⁵ Compared with those complexes which are constructed by three thiacalix[4]arene molecules such as saddle-like $\text{M}^{\text{II}}_{12}$ ($\text{M} = \text{Co}, \text{Ni}$) clusters,³⁸ complexes **1** and **2** here are significantly different due to the change between the bridges in calix[4]arene and thiacalix[4]arene. In general, one calix[4]arene molecule often binds to one TM by its four lower-rim phenolic oxygen atoms and forms a common shuttlecock-like TM-calix[4]arene entity acting as a good molecular building blocks (MBBs). However, with the four bridge sulfur atoms taking part into the coordination, one thiacalix[4]arene molecule can bind to four TMs and simultaneously forms a TM_4 -thiacalix[4]arene MBBs. Both of the abovementioned MBBs can be bridged by different linkers such as metal cations, bridging anions and auxiliary ligands into high nuclearity coordination complexes.

Magnetic studies. The direct current (dc) magnetic susceptibilities were carried out ($H = 1000\text{Oe}$) on the polycrystalline samples of **1** and **2** over 2-300 K. The $\chi_m T$ values at room temperature are 20.16 and 20.81 $\text{cm}^3 \text{K mol}^{-1}$ for **1** and **2**, which are higher than the calculated values of 16.875 $\text{cm}^3 \text{K mol}^{-1}$ ($g = 2$) for 9 uncoupled Co^{II} ions (Figure 6). This can be explained on the unquenched orbital-moment as a consequence of spin-orbital coupling of Co^{II} ions, which is known to be significant in an octahedral field.⁵⁶ Upon cooling to 16.0 K, the $\chi_m T$ value for **1** decreases to 6.29 $\text{cm}^3 \text{K mol}^{-1}$ and abruptly increases to a maximum value of 8.23 $\text{cm}^3 \text{K mol}^{-1} \text{K}$ at 3.0 K, and then decreases until the lowest temperature 2 K. While the $\chi_m T$ product of **2** decreases as the temperature is decreased, and reaches a minimum value of 9.74 $\text{cm}^3 \text{K mol}^{-1} \text{K}$ at 27.0 K, and then decreases to 13.45 $\text{cm}^3 \text{K mol}^{-1}$ at 15.0 K, and then falls rapidly to 2.98 $\text{cm}^3 \text{K mol}^{-1}$ at 2 K. The increases of $\chi_m T$ value for both title complexes at low temperatures (16-3 K for **1**, and 27-15 K for **2**) are suggestive of ferrimagnetic or weak ferromagnetic interactions between the Co^{II} ions, which may be attributed to spin canting antiferromagnetism and/or zero-field splitting of the anisotropic high-spin Co^{II} centers. The reciprocal molar magnetic susceptibility data in the range of 50-300 K obey the Curie-Weiss Law ($1/\chi_m = T/C - \theta/C$)

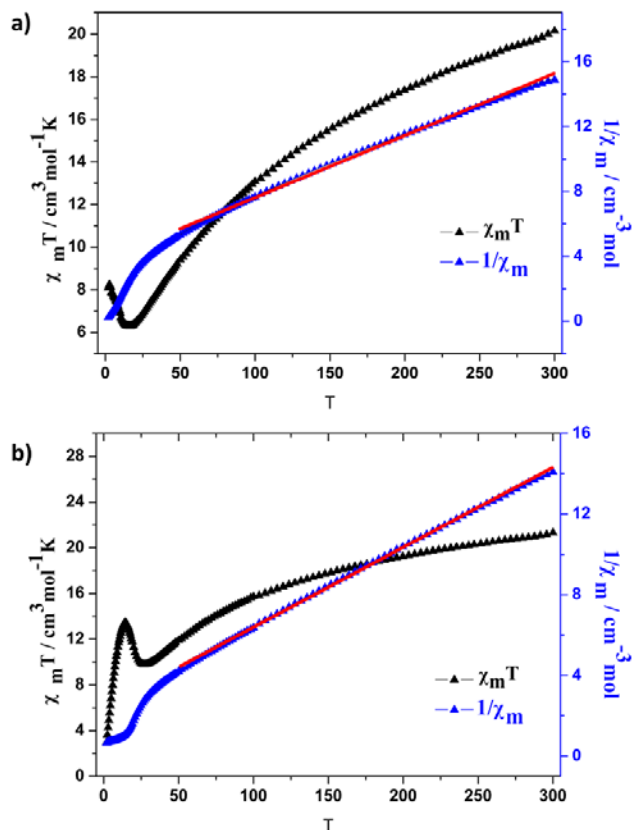


Figure 6. Temperature dependence of magnetic susceptibilities for a) complex **1** and b) complex **2** in a 1000 Oe field. The red solid lines are the best fitting to the Curie-Weiss Law.

with Curie constants (C) of 27.77 and 25.64 and Weiss constants (θ) = -87.75 and -61.54 $\text{cm}^3 \text{K mol}^{-1}$ for complexes **1** and **2**, respectively. However, because of the complicated structure of both title complexes, it is not possible to evaluate the coupling constant between the Co^{II} carriers. The negative Weiss constants and the decrease in the $\chi_m T$ value at high temperature could be arisen from the presence of strong antiferromagnetic interaction between the cobalt ions and/or the spin-orbit coupling effect of Co^{II} .

Field dependence of magnetization (M) versus field (H) data for complexes **1** and **2** are investigated with the applied magnetic field H in the range 0-80 kOe at 2 K (Figures S1 and S2 in the SI). The magnetization of **1** increases quickly at low fields and then more slowly at high fields, while that of **2** increases almost linearly. The magnetization value at the highest field (8 T) is 7.93 and 4.60 $\text{N}\beta$ for complexes **1** and **2** respectively, which is far below the saturation sum value of nine Co^{II} ions. Moreover, no obvious hysteresis loop is observed for both of the complexes at 2 K (Figures S3 and S4 in the SI).

To further characterize the low-temperature behaviors of complexes **1** and **2**, the zero-field-cooled (ZFC) and field-cooled (FC) experiments are performed under a field of 30 Oe in the range of 2-20 K, as shown in Figure 7. Both of the

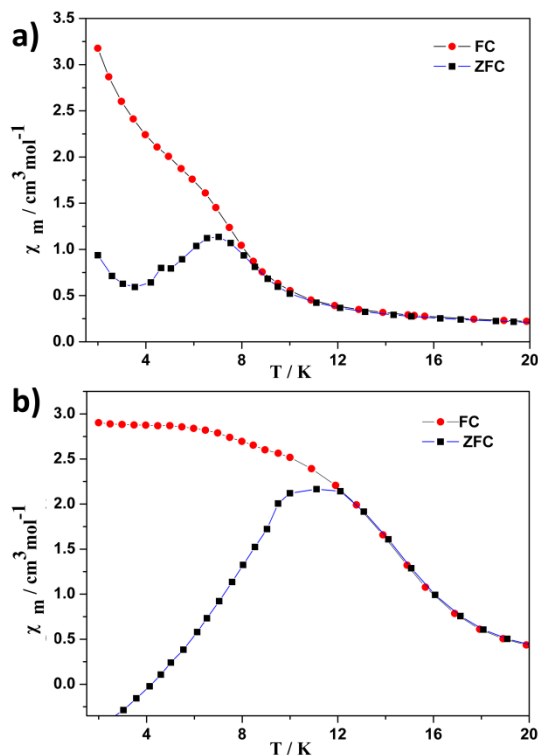


Figure 7. FC and ZFC curves for a) complex **1** and b) complex **2** at an applied field strength of 30 Oe.

complexes show divergences in the low-temperature region (below 8 K for **1**, below 12 K for **2**), which could be caused by spin-glasses, long range-ordered or superparamagnetism. To further confirm the underlying magnetic nature, the temperature dependent alternating current (ac) experiments are performed over 2–20 K with zero dc field and a 3 Oe ac field for both of the complexes as can be seen Figure 8 and 9, respectively. The in-phase and out-of-phase susceptibilities of **1** and **2** both show very small frequency dependence at around 8 and 10 K and the shift parameter values, $\gamma = (\Delta T_B / T_B) / \Delta(\log f)$ ($f = ac$ frequency, $T_B =$ blocking temperature, which is defined as the temperature below which the relaxation of the magnetization becomes slow), are determined to be 0.0236 and 0.0324, which are in the usual range (0.004–0.08) of spin-glass behavior.⁵⁷ According to the above observations, these two calix[4]arene-supported Co^{II} clusters show ferrimagnetic or weak ferromagnetic interactions between the Co^{II} ions at low temperatures with spin-glass behavior, which are different from the reported thiacalix[4]arene-supported cobalt system by our group and Liao's group.^{37-39,40-46} Moreover, the $\chi_m T$, magnetization, spin-glass shift parameter, ZFC and FC of complexes **1** and **2** are also somewhat different. Such different magnetic properties might be due to the introduction of auxiliary phosphate ligand which leads to the changes in the metallic core. Therefore, this work indicates that we may synthesize new complexes with interesting magnetic properties by using different calixarenes and complementary ligands.

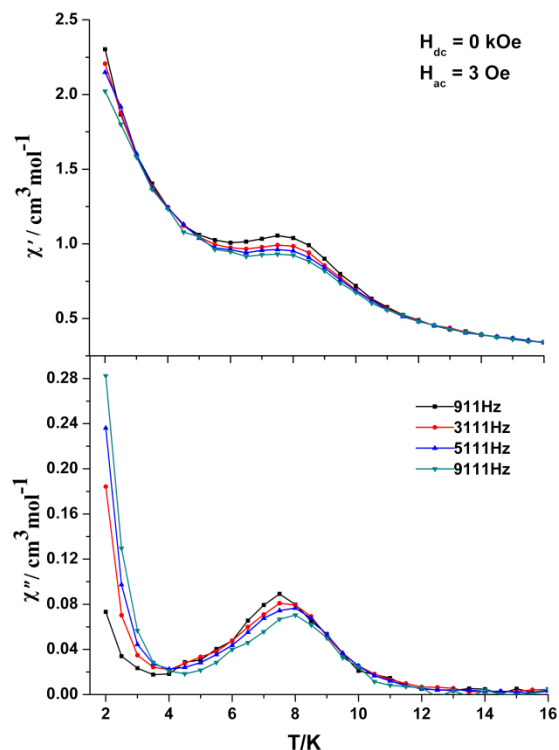


Figure 8. Plot of the in-phase (top) and out-of-phase (bottom) ac susceptibility for **1** in a zero dc field and a 3 Oe ac field.

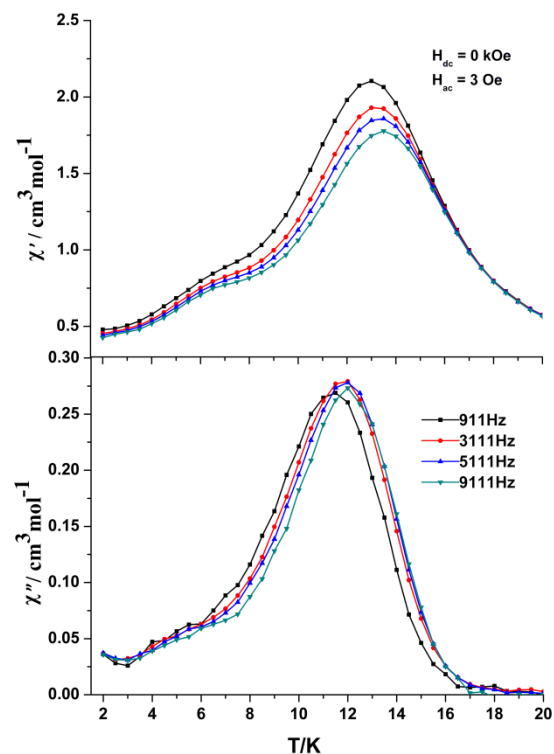


Figure 9. Plot of the in-phase (top) and out-of-phase (bottom) ac susceptibility for **2** in a zero dc field and a 3 Oe ac field.

CONCLUSION

In conclusion, we have formed two new calixarene-supported tri-capped prismatic Co^{II}_9 clusters housing one $\mu_9\text{-CO}_3^{2-}$ anion. In essence, complex **2** is a “distorted” version of complex **1** in which one $\mu_3\text{-OH}$ has been replaced by a much larger μ_3 -bridging phosphonate ligand. As far as we know, they are the first two examples of $\mu_9\text{-CO}_3^{2-}$ bridged paramagnetic metal clusters. Magnetic measurements reveal that both of the complexes display dominant antiferromagnetic interactions (in 50-300 K), ferrimagnetic or weak ferromagnetic exchange (at lower temperatures) and spin-glass behavior. Our future studies will focus on cluster versatility towards different phosphate auxiliary ligands and other metal centers. Such alteration may influence the assembly of the clusters and further influence the magnetic properties.

ACKNOWLEDGMENT

We thank National Natural Foundation of China (21131006) and Deanship of Scientific Research (DSR), King Abdulaziz University, Jeddah, under grant number (1-130-1434-HiCi) for funding this research.

SUPPORTING INFORMATION

Crystallographic data in CIF format, field dependence of magnetization (M) versus field (H) data, the M - H plots, TGA analyses and PXRD patterns for complexes **1** and **2** see online at article link.

REFERENCES AND NOTES

1. T.R. Cook, Y.-R. Zheng, P.J. Stang. Metal-Organic Frameworks and Self-Assembled Supramolecular Coordination Complexes: Comparing and Contrasting the Design, Synthesis, and Functionality of Metal-Organic Materials. *Chem. Rev.* **2013**, 113, 734-77.
2. X. Fang, L. Hansen, F. Haso, P. Yin, A. Pandey, L. Engelhardt, I. Slowing, T. *Liet. al.* {Mo₂₄Fe₁₂} Macrocycles: Anion Templatation with Large Polyoxometalate Guests. *Angew. Chem. Int. Ed.* **2013**, 52, 10500-04.
3. Z. Zhang, L. Wojtas, M.J. Zaworotko. Organic-inorganic hybrid polyhedra that can serve as supermolecular building blocks. *Chemical Science* **2014**.
4. M. Wu, F. Jiang, X. Kong, D. Yuan, L. Long, S.A. Al-Thabaiti, M. Hong. Two polymeric 36-metal pure lanthanide nanosize clusters. *Chemical Science* **2013**, 4, 3104-09.
5. R. Gautier, K. Oka, T. Kihara, N. Kumar, A. Sundaresan, M. Tokunaga, M. Azuma, K.R. Poeppelmeier. Spin Frustration from cis-Edge or -Corner Sharing Metal-Centered Octahedra. *J. Am. Chem. Soc.* **2013**, 135, 19268-74.
6. K. Qian, X.-C. Huang, C. Zhou, X.-Z. You, X.-Y. Wang, K.R. Dunbar. A Single-Molecule Magnet Based on Heptacyanomolybdate with the Highest Energy Barrier for a Cyanide Compound. *J. Am. Chem. Soc.* **2013**, 135, 13302-05.
7. S. Pullen, H. Fei, A. Orthaber, S.M. Cohen, S. Ott. Enhanced Photochemical Hydrogen Production by a Molecular Diiron Catalyst Incorporated into a Metal-Organic Framework. *J. Am. Chem. Soc.* **2013**, 135, 16997-7003.
8. A. Leyva-Pérez, J. Oliver-Meseguer, P. Rubio-Marqués, A. Corma. Water-Stabilized Three- and Four-Atom Palladium Clusters as Highly Active Catalytic Species in Ligand-Free C-C Cross-Coupling Reactions. *Angew. Chem. Int. Ed.* **2013**, 52, 11554-59.
9. E. Coronado, P. Day. Magnetic molecular conductors. *Chem. Rev.* **2004**, 104, 5419-48.
10. J. Yu, Y. Cui, C. Wu, Y. Yang, Z. Wang, M. O'Keeffe, B. Chen, G. Qian. Second-order nonlinear optical activity induced by ordered dipolar chromophores confined in the pores of an anionic metal-organic framework. *Angew. Chem. Int. Ed. Engl.* **2012**, 51, 10542-5.
11. J. Qian, F. Jiang, D. Yuan, X. Li, L. Zhang, K. Su, M. Hong. Increase in pore size and gas uptake capacity in indium-organic framework materials. *Journal of Materials Chemistry A* **2013**, 1, 9075-82.
12. S.S. Mondal, A. Bhunia, A. Kelling, U. Schilde, C. Janiak, H.-J. Holdt. Giant Zn₁₄ Molecular Building Block in Hydrogen-Bonded Network with Permanent Porosity for Gas Uptake. *J. Am. Chem. Soc.* **2013**, 136, 44-47.
13. Z.-F. Liu, M.-F. Wu, F.-K. Zheng, S.-H. Wang, M.-J. Zhang, J. Chen, Y. Xiao, G.-C. Guo, A.Q. Wu. Zinc(ii) coordination compounds based on in situ generated 3-(5H-tetrazol)benzaldehyde with diverse modes: hydrothermal syntheses, crystal structures and photoluminescent properties. *CrystEngComm* **2013**, 15, 7038-47.
14. S. Langley, M. Helliwell, R. Sessoli, S.J. Teat, R.E.P. Winpenny. Synthesis and structural and magnetic characterization of cobalt(II) phosphonate cage compounds. *Inorg. Chem.* **2008**, 47, 497-507.
15. S. Langley, M. Helliwell, R. Sessoli, S.J. Teat, R.E.P. Winpenny. Synthesis and structural and magnetic characterisation of cobalt(II)-sodium phosphonate cage compounds. *Dalton Trans.* **2009**, 3102-10.
16. A.K. Ghosh, M. Pait, M. Shatruk, V. Bertolasi, D. Ray. Self-assembly of a [Ni₈] carbonate cube incorporating four [small mu]4-carbonato linkers through fixation of atmospheric CO₂ by ligated [Ni₂] complexes. *Dalton Trans.* **2014**, 43, 1970-73.
17. M.U. Anwar, Y. Lan, L.M.C. Beltran, R. Clerac, S. Pfirrmann, C.E. Anson, A.K. Powell. In Situ Ligand Transformation in the Synthesis of Manganese Complexes: Mono-, Tri- and a Barrel-shaped Tetradecanuclear Mn-14(II) Aggregate. *Inorg. Chem.* **2009**, 48, 5177-86.
18. S.K. Langley, B. Moubaraki, K.S. Murray. Magnetic Properties of Hexanuclear Lanthanide(III) Clusters Incorporating a Central μ_6 -Carbonate Ligand Derived from Atmospheric CO₂ Fixation. *Inorg. Chem.* **2012**, 51, 3947-49.
19. S. Titos-Padilla, J. Ruiz, J.M. Herrera, E.K. Brechin, W. Wersndorfer, F. Lloret, E. Colacio. Dilution-Triggered SMM Behavior under Zero Field in a Luminescent Zn₂Dy₂ Tetranuclear Complex Incorporating Carbonato-Bridging Ligands Derived from Atmospheric CO₂ Fixation. *Inorg. Chem.* **2013**, 52, 9620-26.
20. S.M. Taylor, S. Sanz, R.D. McIntosh, C.M. Beavers, S.J. Teat, E.K. Brechin, S.J. Dalgarno. p-tert-Butylcalix 8 arene: An Extremely Versatile Platform for Cluster Formation. *Chemistry-a European Journal* **2012**, 18, 16014-22.
21. M. Sarkar, G. Aromi, J. Cano, V. Bertolasi, D. Ray. Double-CO₃²⁻-Centered Co-5(II) Wheel and Modeling of Its Magnetic Properties. *Chemistry-a European Journal* **2010**, 16, 13825-33.
22. A.K. Ghosh, M. Pait, M. Shatruk, V. Bertolasi, D. Ray. Self-assembly of a [Ni₈] carbonate cube incorporating four [small mu]4-carbonato linkers through fixation of atmospheric CO₂ by ligated [Ni₂] complexes. *Dalton Trans.* **2014**.
23. S. Sakamoto, T. Fujinami, K. Nishi, N. Matsumoto, N. Mochida, T. Ishida, Y. Sunatsuki, N. Re. Carbonato-Bridged NiII₂LnIII₂ (LnIII = GdIII, TbIII, DyIII) Complexes Generated by Atmospheric CO₂ Fixation and Their Single-Molecule-Magnet Behavior: [(μ -4-CO₃)₂{NiII(3-MeOsaltN)(MeOH or H₂O)LnIII(NO₃)₂}] • solvent [3-MeOsaltN = N,N'-Bis(3-methoxy-2-oxybenzylidene)-1,3-propanediaminato]. *Inorg. Chem.* **2013**, 52, 7218-29.
24. L. Chen, F. Jiang, M. Wu, N. Li, W. Xu, C. Yan, C. Yue, M. Hong. Half-Open Hollow Cages of Pentadecavanadate and Hexadecavanadate Compounds with Large -O-V-O-V- Windows. *Cryst. Growth Des.* **2008**, 8, 4092-99.
25. K.C. Xiong, F.L. Jiang, Y.L. Gai, Y.F. Zhou, D.Q. Yuan, K.Z. Su, X.Y. Wang, M.C. Hong. A Series of Octanuclear-Nickel(II) Complexes Supported by Thiocalix 4 arenes. *Inorg. Chem.* **2012**, 51, 3283-88.
26. G.J.T. Cooper, G.N. Newton, D.-L. Long, P. Koegler, M.H. Rosnes, M. Keller, L. Cronin. Exploring a Series of Isostructural Dodecanuclear Mixed Ni:Co Clusters: Toward the Control of Elemental Composition Using pH and Stoichiometry. *Inorg. Chem.* **2009**, 48, 1097-104.
27. K.C. Xiong, F.L. Jiang, Y.L. Gai, D.Q. Yuan, D. Han, J. Ma, S.Q. Zhang, M.C. Hong. Chlorine-Induced Assembly of a Cationic Coordination Cage with a μ_5 -Carbonato-Bridged Mn-24(II) Core. *Chemistry-a European Journal* **2012**, 18, 5536-40.

28. K.C. Xiong, X.Y. Wang, F.L. Jiang, Y.L. Gai, W.T. Xu, K.Z. Su, X.J. Li, D.Q. Yuan, M.C. Hong. Heterometallic thiacalix 4 arene-supported Na(2)Ni(12)(II)Ln(2)(III) clusters with vertex-fused tricubane cores (Ln = Dy and Tb). *Chem. Commun.* **2012**, 48, 7456-58.
29. G. Karotsis, S.J. Teat, W. Wernsdorfer, S. Piligkos, S.J. Dalgarno, E.K. Brechin. Calix 4 arene-Based Single-Molecule Magnets. *Angew. Chem. Int. Ed.* **2009**, 48, 8285-88.
30. G. Karotsis, M. Evangelisti, S.J. Dalgarno, E.K. Brechin. A Calix 4 arene 3d/4f Magnetic Cooler. *Angew. Chem. Int. Ed.* **2009**, 48, 9928-31.
31. S.M. Taylor, R.D. McIntosh, S. Piligkos, S.J. Dalgarno, E.K. Brechin. Calixarene-supported clusters: employment of complementary cluster ligands for the construction of a ferromagnetic [Mn5] cage. *Chem Commun* **2012**, 48, 11190-2.
32. C. Aronica, G. Chastanet, E. Zueva, S.A. Borshch, J.M. Clemente-Juan, D. Luneau. A mixed-valence polyoxovanadate(III,IV) cluster with a calixarene cap exhibiting ferromagnetic V(III)-V(IV) interactions. *J. Am. Chem. Soc.* **2008**, 130, 2365-71.
33. C.-M. Liu, D.-Q. Zhang, X. Hao, D.-B. Zhu. Nestlike C4-Symmetric [Co24] Metallamacrocycle Sustained by p-tert-Butylsulfonfylcalix[4]arene and 1,2,4-Triazole. *Chemistry – A European Journal* **2011**, 17, 12285-88.
34. F.-R. Dai, Z. Wang. Modular Assembly of Metal–Organic Supercontainers Incorporating Sulfonfylcalixarenes. *J. Am. Chem. Soc.* **2012**.
35. T. Kajiwara, H.S. Wu, T. Ito, N. Iki, S. Miyano. Octalanthanide wheels supported by p-tert-butylsulfonfylcalix 4 arene. *Angew. Chem. Int. Ed.* **2004**, 43, 1832-35.
36. K.Z. Su, F.L. Jiang, J.J. Qian, M.Y. Wu, K.C. Xiong, Y.L. Gai, M.C. Hong. Thiacalix 4 arene-Supported Kite-Like Heterometallic Tetranuclear Zn(II)Ln(3)(III) (Ln = Gd, Tb, Dy, Ho) Complexes. *Inorg. Chem.* **2013**, 52, 3780-86.
37. K. Su, F. Jiang, J. Qian, M. Wu, Y. Gai, J. Pan, D. Yuan, M. Hong. Open Pentameric Calixarene Nanocage. *Inorg. Chem.* **2013**, 53, 18-20.
38. K.C. Xiong, F.L. Jiang, Y.L. Gai, Z.Z. He, D.Q. Yuan, L. Chen, K.Z. Su, M.C. Hong. Self-Assembly of Thiacalix 4 arene-Supported Nickel(II)/Cobalt(II) Complexes Sustained by in Situ Generated 5-Methyltetrazolate Ligand. *Cryst. Growth Des.* **2012**, 12, 3335-41.
39. K.C. Xiong, F.L. Jiang, Y.L. Gai, D.Q. Yuan, L. Chen, M.Y. Wu, K.Z. Su, M.C. Hong. Truncated octahedral coordination cage incorporating six tetranuclear-metal building blocks and twelve linear edges. *Chemical Science* **2012**, 3, 2321-25.
40. Y.F. Bi, X.T. Wang, W.P. Liao, X.F. Wang, X.W. Wang, H.J. Zhang, S. Gao. A {Co(32)} Nanosphere Supported by p-tert-Butylthiacalix 4 arene. *J. Am. Chem. Soc.* **2009**, 131, 11650-+.
41. Y.F. Bi, W.P. Liao, G.C. Xu, R.P. Deng, M.Y. Wang, Z.J. Wu, S. Gao, H.J. Zhang. Three p-tert-Butylthiacalix 4 arene-Supported Cobalt Compounds Obtained in One Pot Involving In Situ Formation of N(6)H(2) Ligand. *Inorg. Chem.* **2010**, 49, 7735-40.
42. Y.F. Bi, G.C. Xu, W.P. Liao, S.C. Du, X.W. Wang, R.P. Deng, H.J. Zhang, S. Gao. Making a Co(24) metallamacrocycle from the shuttlecock-like tetranuclear cobalt-calixarene building blocks. *Chem. Commun.* **2010**, 46, 6362-64.
43. M. Liu, W. Liao, C. Hu, S. Du, H. Zhang. Calixarene-Based Nanoscale Coordination Cages. *Angew. Chem. Int. Ed.* **2012**, 51, 1585-88.
44. A Tetragonal Prismatic {Co32} Nanocage Based on Thiacalixarene. *CC* **2013**.
45. Y. Bi, S. Wang, M. Liu, S. Du, W. Liao. A tetragonal prismatic {Co32} nanocage based on thiacalixarene. *Chem. Commun.* **2013**, 49, 6785-87.
46. W. Liu, M. Liu, S. Du, Y. Li, W. Liao. Bridging cobalt - calixarene subunits into a Co8 entity or a chain with 4,4' -bipyridyl. *J. Mol. Struct.* **2014**, 1060, 58-62.
47. M.M. Olmstead, G. Sigel, H. Hope, X.J. Xu, P.P. Power. Metallocalixarenes - syntheses and x-ray crystal-structures of titanium(iv), iron(iii), and cobalt(ii) complexes of para-tert-butylcalix 4 arene. *J. Am. Chem. Soc.* **1985**, 107, 8087-91.
48. W. Liu, H.H. Thorp. Bond valence sum analysis of metal-ligand bond lengths in metalloenzymes and model complexes. 2. Refined distances and other enzymes. *Inorg. Chem.* **1993**, 32, 4102-05.
49. C.D. Gutsche, M. Iqbal, D. Stewart. Calixarenes .18. Synthesis procedures for para-tert-butylcalix 4 arene. *J. Org. Chem.* **1986**, 51, 742-45.
50. CrystalClear Version 1.3.6, RIGAKU/MSC(2004), Rigaku/MS, 9009 New Trails Drive, The Woodlands, TX77381-5209, USA.
51. (a) G. M. Sheldrick, SHELXS 97, Program for crystal Structure Solution, **1997**, University of Göttingen. (b) G. M. Sheldrick, SHELXL 97, Program for crystal Structure Refinement, **1997**, University of Göttingen.
52. P. van der Sluis, A.L. Spek. BYPASS: an effective method for the refinement of crystal structures containing disordered solvent regions. *Acta Crystallographica Section A* **1990**, 46, 194-201.
53. S.D. Bian, J.H. Jia, Q.M. Wang. High-Nuclearity Silver Clusters Templated by Carbonates Generated from Atmospheric Carbon Dioxide Fixation. *J. Am. Chem. Soc.* **2009**, 131, 3422-3423.
54. K. Hyva`rinen, M. Klinga, M. Leskela`. Synthesis and crystal structure of a novel multiple bridged cubane type (Li4O3Cl)3 lithium carbonate chloro HMPA siloxane complex, [[Li4(μ3-Cl)(μ6-OSi(CH3)2O(CH3)2SiO) (μ-OP(N(CH3)2)3)(OP(N(CH3)2)3)]3(μ3-Cl)(μ9-CO3)]·2C4H8O. *Polyhedron* **1996**, 15, 2171-77.
55. G. Karotsis, S. Kennedy, S.J. Dalgarno, E.K. Brechin. Calixarene supported enneanuclear Cu(II) clusters. *Chem. Commun.* **2010**, 46, 3884-86.
56. M.A.M. Abu-Youssef, F.A. Mautner, R. Vicente. 1D and 2D End-to-End Azide-Bridged Cobalt(II) Complexes: Syntheses, Crystal Structures, and Magnetic Properties. *Inorg. Chem.* **2007**, 46, 4654-59.
57. J. A. Mydosh, Spin Glasses: An Experimental Introduction; Taylor & Francis: London, **1993**.